

Analytic impurity solver with the Kondo strong-coupling asymptotics

V. Janiš and P. Augustinský

*Institute of Physics, Academy of Sciences of the Czech Republic,
Na Slovance 2, CZ-18221 Praha 8, Czech Republic**

(Dated: May 3, 2019)

We present an analytic universal impurity solver for strongly correlated electrons. We extend the many-body perturbation expansion via suitable two-particle renormalizations from the Fermi-liquid regime to the critical region of the metal-insulator transition. The reliability of the approximation in the strong-coupling limit is demonstrated by reproducing the Kondo scale in the single-impurity Anderson model. We disclose the origin of the Kondo resonance in terms of Feynman diagrams and find criteria for the existence of the proper Kondo asymptotic behavior in approximate theories.

PACS numbers: 72.15.Qm, 75.20.Hr

I. INTRODUCTION

One must have at hand a reliable theory capturing the salient features of the strong-coupling asymptotics to comprehend fully the effects of electron correlations in metals. Most theoretical approaches are based on the well established weak-coupling expansion and we have only a few opportunities to test its extensions to the strong-coupling regime. The most reliable check of credibility of a theory in the strong-coupling regime is to compare its results with one of the existing exact solutions in this limit. There are two principal exact results for strongly correlated electrons. It is the single-impurity Anderson model (SIAM) and the $1d$ Hubbard model. The ground state of both models at half filling was constructed with the aid of the Bethe ansatz. The former is a heavy-fermion liquid in the strong-coupling limit,¹ while the latter is an electron-hole liquid for arbitrary interaction strength.²

Recently SIAM has won on importance, since its solutions form a fundamental building block in the construction of a dynamical mean-field theory (DMFT) of strong electron correlations via the limit to infinite-dimensional lattices.³ Unfortunately, there are only approximate impurity solvers in the strong-coupling regime. The only analytic theory, non-crossing approximation, is not a Fermi liquid and displays low-energy pathological features.⁴ Numerical quantum Monte-Carlo simulations⁵ are restricted to rather high temperatures. The most reliable impurity solver proved to be the numerical renormalization group. It produces the expected three-peak spectral function with the central Kondo resonance for intermediate coupling.^{6,7} Due to limitations of the numerical procedure it cannot be extended to arbitrarily large interactions. Neither of these solutions, however, is capable to produce a detailed ultimate picture of the the strong-coupling limit and to decide whether and in which form the Kondo resonance survives or whether the system undergoes a metal-insulator transition. This question can only be answered by an analytically controlled theory.

There is presently no global analytic theory capable of tracing down the genesis of the correlation-induced

Kondo resonance. The standard weak-coupling, Fermi-liquid-based perturbation expansion renormalized with various self-energy insertions becomes unstable for intermediate and strong electron interaction.⁸ Attempts to go beyond one-particle renormalizations by introducing explicit vertex corrections and a two-particle self-consistency either do not lead to analytically solvable equations or have not yet produced the desired Kondo asymptotics in SIAM.^{9,10}

The aim of this paper is to construct an analytically controllable approximation that would reliably interpolate between the weak- and strong-coupling regimes in models with a screened electron repulsion. To this purpose we use an appropriately renormalized diagrammatic many-body expansion. We demonstrate that it is not the one-particle self-consistency but rather a two-particle one that must be introduced in the critical region of the metal-insulator transition. We further show that only a symmetric inclusion of electron-electron and electron-hole scatterings leads to the proper critical behavior. The two-particle self-consistency will be achieved within the parquet approximation in which we separate singular and regular functions. Not to lose analytic control only the potentially divergent functions with long-range fluctuations are kept dynamical while the regular ones with short-range fluctuations are replaced by constants. Such a simplification does not affect the universal features of the critical behavior. We explicitly construct the approximation for SIAM so that its reliability becomes transparent by qualitatively correctly reproducing the exact weak-coupling (Fermi-liquid) and strong-coupling (Kondo) regimes. We identify with our construction the minimal necessary conditions on approximate schemes to cover the Kondo strong-coupling behavior.

II. MODEL AND BASIC EQUATIONS

We formulate the construction of an approximate theory interpolating between the weak and strong coupling regimes independently of the underlying model via renormalized Feynman diagrams and equations of motion. To demonstrate reliability of our approach we, however, use

in our explicit calculations the single impurity Anderson model the Hamiltonian of which reads

$$\hat{H} = \sum_{\mathbf{k}\sigma} \epsilon(\mathbf{k}) c_{\mathbf{k}\sigma}^\dagger c_{\mathbf{k}\sigma} + E_d \sum_{\sigma} d_{\sigma}^\dagger d_{\sigma} + \sum_{\mathbf{k}\sigma} \left(V_{\mathbf{k}} d_{\sigma}^\dagger c_{\mathbf{k}\sigma} + V_{\mathbf{k}}^* c_{\mathbf{k}\sigma}^\dagger d_{\sigma} \right) + U \hat{n}_{\uparrow}^d \hat{n}_{\downarrow}^d. \quad (1)$$

We denoted $\hat{n}_{\sigma}^d = d_{\sigma}^\dagger d_{\sigma}$. When calculating the grand potential and thermodynamic properties of this impurity model we can explicitly integrate over the degrees of freedom of the delocalized electrons. To this purpose we standardly replace the local part of the propagator of the mobile electrons by a constant $\Delta(\epsilon) = \pi \sum_{\mathbf{k}} |V_{\mathbf{k}}|^2 \delta(\epsilon - \epsilon(\mathbf{k})) \doteq \Delta$ the value of which we set as the energy unit. For simplicity we assume half-filled case $\mu = E_d + U/2$. The impurity grand partition function can then be represented via a local Grassmann functional integral

$$\mathcal{Z} = \int \mathcal{D}\psi \mathcal{D}\psi^* \exp \left\{ \sum_n \psi_n^*(i\omega_n + \bar{\mu} + i\text{sign}(\omega_n)\Delta) \psi_n - U \int_0^{\beta} d\tau \hat{n}_{\uparrow}^d(\tau) \hat{n}_{\downarrow}^d(\tau) \right\}. \quad (2)$$

For this integral we can straightforwardly build up the standard weak-coupling (diagrammatic) perturbation expansion in powers of the interaction strength U (diagrammatically represented as a vertex) and the bare propagator, being in the impurity case $G_0(x + iy) = 1/(x + i\text{sign}(y)(\Delta + |y|))$ (diagrammatically represented as an oriented line).

We know that in the particular case of SIAM the non-renormalized weak-coupling expansion is preferred and converges for arbitrary interaction strength.¹¹ To enable a treatment of phase transitions and singularities in more general extended lattice models we have, however, to renormalize the bare expansion. The fundamental quantity for renormalization in the many-body perturbation expansion is the self-energy. In our approach we do not use the self-energy as the approximation-generating quantity determined directly from sums of selected (renormalized) diagrams. Instead, we represent it by means of the Schwinger-Dyson equation and the two-particle vertex Γ as follows

$$\Sigma_{\sigma}(i\omega_n) = \frac{U}{\beta} \sum_{n'} G_{-\sigma}(i\omega_{n'}) \left[1 - \frac{1}{\beta} \sum_m G_{\sigma}(i\omega_{n+m}) \times G_{-\sigma}(i\omega_{n'+m}) \Gamma_{\sigma-\sigma}(i\omega_{n+m}; i\omega_n, i\nu_{n'-n}) \right] \quad (3)$$

where $\omega_n = (2n + 1)\pi T$ and $\nu_m = 2\pi m T$ are fermionic and bosonic Matsubara frequencies in units $k_B = 1$, respectively. We assigned dynamical variables to the two-particle vertex as shown in Fig. 1.

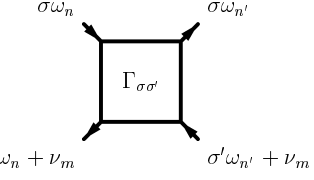


FIG. 1: Diagrammatic assigning of dynamical variables, frequencies and spins, to the vertex $\Gamma_{\sigma\sigma'}(i\omega_n, i\omega_{n'}; i\nu_m)$.

We further introduce two-particle irreducible vertices, that is, vertices that cannot be diagrammatically disconnected by cutting specific pairs of one-particle lines (propagators). The choice of the two-particle irreducibility is ambiguous.¹² Here we choose only the singlet electron-hole and electron-electron scattering channels. We denote the respective irreducible vertices Λ^{eh} and Λ^{ee} . With their aid we represent the full two-particle vertex via two nonequivalent Bethe-Salpeter (BS) equations. The Bethe-Salpeter equation in the eh channel reads

$$\begin{aligned} \Gamma_{\uparrow\downarrow}(i\omega_n, i\omega_{n'}, i\nu_m) &= \Lambda_{\uparrow\downarrow}^{eh}(i\omega_n, i\omega_{n'}, i\nu_m) \\ &- \frac{1}{\beta} \sum_{n''} \Lambda_{\uparrow\downarrow}^{eh}(i\omega_n, i\omega_{n'}; i\nu_m) G_{\uparrow}(i\omega_{n''}) G_{\downarrow}(i\omega_{n''+m}) \\ &\times \Gamma_{\uparrow\downarrow}(i\omega_{n''}, i\omega_{n'}; i\nu_m). \end{aligned} \quad (4a)$$

In the ee channel we obtain

$$\begin{aligned} \Gamma_{\uparrow\downarrow}(i\omega_n, i\omega_{n'}; i\nu_m) &= \Lambda_{\uparrow\downarrow}^{ee}(i\omega_n, i\omega_{n'}; i\nu_m) \\ &- \frac{1}{\beta} \sum_{n''} \Lambda_{\uparrow\downarrow}^{ee}(i\omega_n, i\omega_{n''}; i\nu_{m+n'-n''}) G_{\uparrow}(i\omega_{n''}) \\ &\times G_{\downarrow}(i\omega_{n+n'+m-n''}) \Gamma_{\uparrow\downarrow}(i\omega_{n''}, i\omega_{n'}; i\nu_{m+n-n''}). \end{aligned} \quad (4b)$$

Equations (3) and (4) reduce the solution of the investigated model to the determination of the irreducible vertices Λ^{eh} and Λ^{ee} . The principal idea of the parquet approach is to use the topological nonequivalence of different Bethe-Salpeter representations of the full two-particle vertex via the irreducible ones. Due to the nonequivalence of different types of two-particle scatterings the reducible vertex in one channel is irreducible in the other one.¹² If the vertex irreducible in both channels is the bare interaction U (parquet approximation) we obtain the basic parquet equation in our two-channel scheme

$$\Gamma_{\uparrow\downarrow} = \Lambda_{\uparrow\downarrow}^{eh} + \Lambda_{\uparrow\downarrow}^{ee} - U. \quad (5)$$

We use this representation in Eqs. (4) to exclude the full vertex Γ from the BS equations that then become coupled convolutive nonlinear integral equations for the irreducible vertices Λ^{eh} and Λ^{ee} . These equations cannot be solved analytically and their numerical solution is available only far from the Kondo regime.¹³ To gain an analytic assessment of the low-temperature, strong-coupling behavior of the parquet equations (4) using Eq. (5) we have to resort to simplifications.

III. KONDO ASYMPTOTICS – VERTEX FUNCTIONS

A. Simplified parquet equations

Equations (4) can be analytically solved (in an approximate way) individually for the full vertex Γ by neglecting Eq. (5) and using the irreducible vertices as input. Approximations of this type with renormalized one-particle propagators are now called fluctuation-exchange (FLEX). In the simplest case the irreducible vertices are replaced by the bare interaction. We find that vertex Γ tends to develop a pole in the BS equation with multiple electron-hole scatterings, Eq. (4a), caused by the imminent metal-insulator transition at zero temperature. While the two-particle vertex Γ remains finite (bounded) when calculated from Eq. (4b). We use the fact that only equation (4a) develops a pole in simplifying the parquet approximation in the critical region of the metal-insulator transition to an analytically controllable theory. Since the output of the BS equation from one channel enters the kernel of the other one, only Λ^{ee} becomes singular in the critical region of the metal-insulator transition. The irreducible vertex Λ^{eh} remains bounded everywhere in the parquet approximation.

We restrict our interest to the leading critical behavior of the solution of the parquet equations in the asymptotic region of the metal-insulator transition. To this purpose we use the reasoning of the renormalization group and neglect the short-range fluctuations. We take into account explicitly only long-range (in time) fluctuations shaping the singular behavior. In this way we do not influence the universal part of the critical asymptotics. We hence keep only singular functions dynamical (dependent on the relevant frequency only). Regular functions, where only short-range fluctuations contribute, can be replaced by constants, suitably chosen averaged values. We must further guarantee that only the leading low-frequency behavior of singular functions determines the critical behavior in the Bethe-Salpeter equations.

As a first step we approximate Λ^{eh} with a static effective interaction $\Lambda^{eh} = \bar{U}$. Inserting this ansatz into Eq. (4a) we obtain a FLEX-type equation for the irreducible vertex from the electron-electron channel

$$\Lambda_{\uparrow\downarrow}^{ee}(i\omega_n, i\omega_{n'}; i\nu_m) = U - \frac{\bar{U}^2 \chi_{eh}(i\nu_m)}{1 + \bar{U} \chi_{eh}(i\nu_m)} \quad (6a)$$

where we denoted the electron-hole bubble $\chi_{eh}(i\nu_m) = \beta^{-1} \sum_n G_{\uparrow}(i\omega_n) G_{\downarrow}(i\omega_{n+m})$. Since the static approximation to the electron-hole irreducible vertex $\Lambda^{eh} = \bar{U}$ causes a deviation from the exact high-frequency limit $\Lambda^{eh} \rightarrow U$, approximation (6a) holds in the low-frequency limit. We hence have to consider in our simplification only the leading low-frequency contribution from the

right-hand side of Eq. (6a). It reads

$$\Lambda_{\uparrow\downarrow}^{sing}(i\nu_m) = - \frac{\bar{U}^2 \chi_{eh}(i\nu_m)}{1 + \bar{U} \chi_{eh}(i\nu_m)}. \quad (6b)$$

We now use Eqs. (4b) and (5), and Λ^{sing} from Eq. (6b) to determine the effective interaction \bar{U} . The right-hand side of Eq. (4b) remains frequency-dependent even with our ansatz. Since we neglect all finite (short-time) fluctuations in regular functions, we have to replace the vertex Γ resulting from Eq. (4b) with a constant. This replacement is not uniquely defined but the ambiguity has no impact on the qualitative (universal) critical behavior of the solution. We found that the most appropriate way in replacing the full vertex with a constant is to multiply both sides of Eq. (4b) with pairs of one-electron propagators $G(i\omega_n)G(i\omega_{m-n})$ from the left and by $G(i\omega_{n'})G(i\omega_{m-n'})$ from the right. We then average over the fermionic Matsubara frequencies with a constraint $m = 0$, conserved during the electron-electron multiple scatterings. Doing so we obtain an explicit equation for the effective interaction, the static part of the electron-hole irreducible vertex,

$$\bar{U} \chi_{ee}(0) = U \chi_{ee} - \frac{\langle G_{\uparrow} G_{\downarrow} L_{\uparrow\downarrow}^2 \rangle}{\chi_{ee} + \langle G_{\uparrow} G_{\downarrow} L_{\uparrow\downarrow} \rangle}. \quad (7)$$

We denoted $\chi_{ee} = \beta^{-1} \sum_n G_{\uparrow}(i\omega_n) G_{\downarrow}(i\omega_{-n})$ the static part of the electron-electron bubble and

$$L_{\uparrow\downarrow}(i\omega_n) = \frac{1}{\beta} \sum_{n'} G_{\uparrow}(i\omega_{n'}) G_{\downarrow}(i\omega_{-n'}) \Lambda_{\uparrow\downarrow}^{sing}(i\nu_{-n-n'}), \quad (8a)$$

$$\langle G_{\uparrow} G_{\downarrow} X \rangle = \frac{1}{\beta} \sum_n G_{\uparrow}(i\omega_n) G_{\downarrow}(i\omega_{-n}) X(i\omega_n). \quad (8b)$$

Equations (6b) - (8) form a closed set of relations determining the static effective interaction \bar{U} and the dynamical vertex $\Lambda_{\uparrow\downarrow}^{sing}(i\nu_m)$ as functionals of the one-particle propagators G_{σ} and the bare interaction U . Together with Eqs. (5) and (3) we have an analytic approximation in closed form. The one-electron propagators may be either bare or renormalized with the self-energy, when one-particle self-consistency is used. The latter is not mandatory and we show that it worsens the approximation with the Hartree one-electron propagators, in particular in the intermediate and high-frequency sectors.

The critical region of the metal-insulator transition in SIAM corresponds to the strong-coupling regime, $U/\Delta \rightarrow \infty$. It is reached when the denominator on the r.h.s. of Eq. (6b) approaches zero. At zero temperature, half filling, and in the rotationally invariant case, $G_{\uparrow} = G_{\downarrow}$ we define a dimensionless Kondo scale $a = 1 + \bar{U} \chi_{eh}(0) = 1 - \bar{U} \int_{-\infty}^0 d\omega \Im[G_{\pm}(\omega)^2]/\pi \rightarrow 0$. We used an abbreviation $G_{\pm}(\omega) \equiv G(\omega \pm i0^+)$. The denominator of the r.h.s. of Eq. (6b) can then be expanded only to the lowest (linear) order in frequency if

we are interested in the leading singular behavior. We obtain $1 + \overline{U}\chi_{eh}(\omega + i0^+) = a - i\pi\overline{U}\rho_0^2\omega$. We denoted the density of one-particle states at the Fermi energy $\rho_0 = -\pi^{-1}\Im G_+(0)$. It does not depend at zero temperature and half filling on the interaction strength. This singular low-frequency asymptotics of Λ^{sing} allows us to evaluate the leading contributions to the integrals in Eqs. (8).

The leading contributions to the integrals with vertex Λ^{sing} in the asymptotic limit $a \rightarrow 0$ read

$$L_{\uparrow\downarrow}(z) \doteq \frac{G(z)G(-z)}{\pi^2\rho_0^2} |\ln a| , \quad (9a)$$

$$\begin{aligned} & \langle G_{\uparrow}G_{\downarrow}L_{\uparrow\downarrow} \rangle \\ & \doteq -\left(\frac{|\ln a|}{\pi^2\rho_0^2}\right) \int_{-\infty}^0 \frac{d\omega}{\pi} \Im [G_+(\omega)^2 G_-(-\omega)^2] , \end{aligned} \quad (9b)$$

and

$$\begin{aligned} & \langle G_{\uparrow}G_{\downarrow}L_{\uparrow\downarrow}^2 \rangle \\ & \doteq -\left(\frac{|\ln a|}{\pi^2\rho_0^2}\right)^2 \int_{-\infty}^0 \frac{d\omega}{\pi} \Im [G_+(\omega)^3 G_-(-\omega)^3] . \end{aligned} \quad (9c)$$

The effective interaction has an asymptotic solution for $a \rightarrow 0$

$$\overline{U} = \frac{1}{\chi_{ee}} \left[U\chi_{ee} - \frac{|\ln a|}{\pi^2\rho_0^2} \frac{\langle (GG)_{ee}^3 \rangle}{\langle (GG)_{ee}^2 \rangle} \right] \quad (10)$$

where we denoted $\langle (GG)_{ee}^n \rangle = -\pi^{-1} \int_{-\infty}^0 d\omega \Im [G_+(\omega)^n G_-(-\omega)^n]$.

The dimensionless Kondo scale measuring the distance from the metal-insulator transition is determined from an equation for the critical point of the metal-insulator transition. It reads $1 + \overline{U}\chi_{eh}(0) = 0$. At half filling $\chi_{eh}(0) = -\chi_{ee}$ and we obtain a leading-order asymptotic solution for the distance to the critical point

$$a = \exp \left\{ -\pi^2\rho_0^2 \frac{\langle (GG)_{ee}^2 \rangle}{\langle (GG)_{ee}^3 \rangle} [U\chi_{ee} - 1] \right\} . \quad (11)$$

Solution (11) holds at zero temperature and half filling when the argument in the exponential tends to infinity and $U\chi_{ee} > 1$. The latter condition can be viewed as a characteristic of the strong-coupling regime, since the FLEX, weak-coupling solutions are distinguished by the opposite inequality, $U\chi_{ee} < 1$.

B. Hartree propagators

To manifest analytically that Eq. (11) reproduces correctly the Kondo asymptotics we use the bare (Hartree) one-particle propagators in Eq. (11). In this case the integrals with powers of the one-particle propagators can be

explicitly evaluated, $\langle (GG)_{ee}^n \rangle = \pi^{2(n-1)}\rho_0^{(2n-1)}/(2n-1)$. Using this result we obtain an explicit representation for the Kondo scale

$$a = \exp \left\{ -\frac{5}{3} [U\rho_0 - 1] \right\} . \quad (12)$$

The exact result is $a = \exp\{-\pi^2 U\rho_0/8\}$. Determination of the exact prefactor at the linear dependence of the exponent of the Kondo scale on the interaction strength is beyond the reach of the present approximation. The prefactor depends on the way in which we replace regular frequency-dependent functions with constants. The universal feature of the Kondo scale is *linearity* in the interaction strength of the exponent. This linearity is the major achievement of our construction. The other Fermi-liquid-based approximations fail in the strong-coupling regime of SIAM. The single-channel FLEX-type approximations either do not see the metal-insulator transition at all (ee channel) or predict a quadratic exponent $a \sim \exp\{-U^2\rho_0^2\}$ (eh channels).¹⁴

IV. KONDO ASYMPTOTICS – ONE-PARTICLE FUNCTIONS

The core of the parquet approach is a self-consistency determining the two-particle irreducible vertices from the completely irreducible vertex (bare interaction in the parquet approximation) and the one-particle propagators. Both, the completely irreducible vertex and the one-particle propagators serve as input to the parquet equations. To complete the parquet approximation and make it conserving and thermodynamically consistent we have to determine the physical one-particle functions, that is, the physical one-particle propagator and the self-energy. All physical quantities in conserving theories are then generated from the full one-particle propagator or the self-energy and their dependence on appropriate external sources.¹⁵ The physical one-particle propagator need not be identical with the "auxiliary" one used in the parquet equations for the two-particle vertices.

A. Self-energy in the parquet approach

The fundamental quantity for any thermodynamically consistent and conserving approximation is the self-energy. Knowing the full two-particle vertex from the parquet equations we determine the self-energy from the Schrödinger-Dyson equation (3). It reduces in the critical region of the metal-insulator transition to a simple FLEX-type expression

$$\Sigma_{\sigma}(i\omega_n) = \frac{U}{\beta} \sum_{n'} \frac{G_{-\sigma}(i\omega_{n'})}{1 + \overline{U}\chi_{eh}(i\nu_{n-n'})} . \quad (13)$$

We can analytically continue the sum over Matsubara frequencies to an integral with Fermi function. At zero

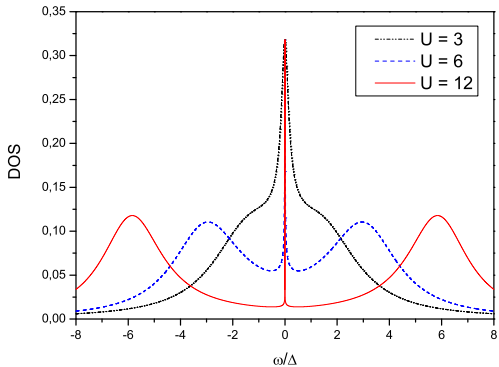


FIG. 2: (Color online) Density of states at zero temperature, half filling, and various interaction strengths without one-particle self-consistency.

temperature the real part of the self-energy reads

$$\begin{aligned}
 & \Re\Sigma_+(\omega) \\
 &= -U \left[\theta(\omega) \int_{-\infty}^{-\omega} + \theta(-\omega) \int_{-\infty}^0 \right] \frac{dx}{\pi} \Im \frac{G_+(x+\omega)}{1 + \overline{U}\chi_+(x)} \\
 &\quad - U\theta(\omega) \int_{-\omega}^0 \frac{dx}{\pi} \Re G_+(x+\omega) \Im \frac{1}{1 + \overline{U}\chi_+(x)} \\
 &\quad - U\theta(-\omega) \int_0^{-\omega} \frac{dx}{\pi} \Im G_+(x+\omega) \Re \frac{1}{1 + \overline{U}\chi_+(x)} . \quad (14a)
 \end{aligned}$$

The imaginary part has a representation

$$\begin{aligned}
 \Im\Sigma_+(\omega) &= -U \left[\theta(\omega) \int_{-\omega}^0 + \theta(-\omega) \int_0^{-\omega} \right] \frac{dx}{\pi} \\
 &\quad \Im G_+(x+\omega) \Im \frac{1}{1 + \overline{U}\chi_+(x)} . \quad (14b)
 \end{aligned}$$

We distinguished with a subscript + the way the real frequency axis is approached in functions with complex variables. That is, $G_+(x) \equiv G(x + i0^+)$, $\chi_+(x) \equiv \chi_{eh}(x + i0^+)$. The one-particle propagators on the r.h.s. of Eqs. (14) may either be bare or full propagators with the self-energy from the left-hand side. Both constructions lead to conserving approximations when all thermodynamic quantities are determined from the self-energy.

We first use the bare (Hartree) one-particle propagators in Eqs. (14). The density of states calculated from the one-particle propagator containing the self-energy from Eq. (14) is plotted for various interaction strengths in Fig. 2. The central Kondo quasiparticle is well formed and its width shrinks with increasing interaction strength in accord with Eq. (12). See Fig. 3 for a detailed dependence of the quasiparticle peak on the interaction strength. Not only the central quasiparticle peak but also the satellite Hubbard bands are well formed. Even though our approximation was justified for small frequen-

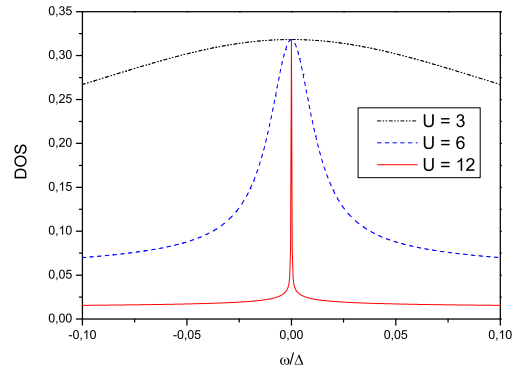


FIG. 3: (Color online) Detailed dependence of the quasiparticle peak in the density of states on the interaction strength.

cies, the parquet equations with the Hartree propagators reproduce the high-frequency features of the spectral function surprisingly well. The Hubbard bands are positioned very close to the exact values of the atomic levels of the impurity electrons at $\pm U/2$.

B. One-particle self-consistency

Usage of the Hartree propagators may seem inferior to a theory with renormalized one-particle propagators in the parquet equations. In fact, the opposite is true, even though the one-particle self-consistency adds new self-energy diagrams to those explicitly taken into account in the parquet construction of the self-energy from the two-particle vertex. The solution with renormalized one-particle propagators loses most of attractive features obtained in the parquet approach with the Hartree propagators. First, the asymptotic formula for the Kondo scale, Eq. (11) cannot be evaluated explicitly when renormalized one-particle propagators are used. Hence, the exact strong-coupling asymptotics cannot be reached analytically. Second, the satellite peaks are completely washed out and merge with the central quasiparticle peak of the density of states as shown in Fig. 4. The central peak broadens with respect to the solution with the Hartree propagators. The solution with renormalized one-particle propagators shows overall worse agreement with the exact Kondo behavior derived from the Bethe ansatz. An analogous behavior was observed in a static simplification of the parquet equations.¹⁶ The failure of one-particle self-consistent theories to reproduce reliably the Kondo strong-coupling regime in impurity models is in accord with early analyses of SIAM using perturbation expansion in the interaction strength.¹¹

The density of states resulting from the parquet approximation with renormalized one-particle propagators resembles the solution of the renormalized RPA of

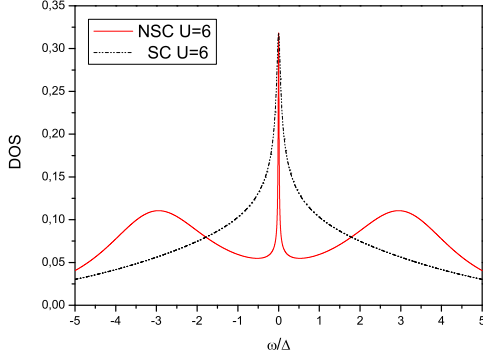


FIG. 4: (Color online) Density of states for one-particle non-self-consistent (NSC) and self-consistent (SC) solutions compared.

Suhl.¹⁷ The central quasiparticle peak is, however, much broader than in the FLEX-type approximations. It is even broader than that from the parquet solution with the Hartree propagators. This indicates that the critical region of the metal-insulator transition is reached, if ever, for much stronger interactions in the solution with one-particle self-consistency than without it. The high-frequency behavior of the parquet approximation with renormalized one-particle propagators and the FLEX solution seem to behave similarly. One can prove analytically that the one-particle self-consistent theories with simplified one-frequency two-particle vertex functions behave in the high-frequency region universally and no Hubbard satellite bands emerge.

To assess the high-frequency behavior of one-particle propagators we evaluate explicitly the leading-order contribution to the self-energy in the critical region of the metal-insulator transition, that is, $a \rightarrow 0$. We obtain from Eqs. (14)

$$\Re\Sigma_+(\omega) \doteq \frac{U}{\bar{U}\pi^2\rho_0^2} \left[|\ln a| \Re G_+(\omega) + \arctan\left(\frac{\bar{U}\pi\rho_0^2\omega}{a}\right) \Im G_+(\omega) \right], \quad (15a)$$

$$\Im\Sigma_+(\omega) \doteq \frac{U}{2\bar{U}\pi^2\rho_0^2} \ln \left[1 + \frac{\bar{U}^2\pi^2\rho_0^4\omega^2}{a^2} \right] \Im G_+(\omega). \quad (15b)$$

If we now assume $\omega \gg a\Delta$ we can further simplify the expression for the self-energy to

$$\tilde{\Sigma}_+(\omega) = \frac{U|\ln a|}{\bar{U}\pi^2\rho_0^2} \left[\tilde{G}_+(\omega) + \frac{\pi \text{sign}(\omega)}{2|\ln a|} \Im \tilde{G}_+(\omega) \right]. \quad (16)$$

We decorated the high-frequency one-particle quantities with tilde to distinguish them from the full ones. For tilde functions we can introduce a dimensionless variable

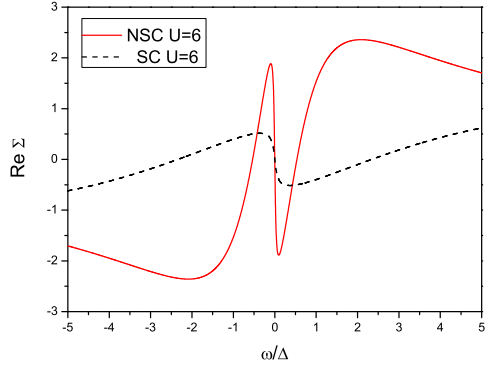


FIG. 5: (Color online) Real part of the self-energy for one-particle non-self-consistent (NSC) and self-consistent (SC) solutions compared.

$$x = \sqrt{\frac{\bar{U}\pi^2\rho_0^2}{U|\ln a|}} \omega. \quad (17a)$$

We resolve the one-electron tilde propagator by using the Dyson equation of SIAM. We obtain an explicit solution

$$\tilde{G}_+(\omega) = \sqrt{\frac{\bar{U}\pi^2\rho_0^2}{U|\ln a|}} \left[\frac{x}{2} - i\sqrt{1 - \frac{x^2}{4}} \right]. \quad (17b)$$

We see that one-particle self-consistent theories lead to a universal high-frequency behavior with a semi-elliptic density of states spread over a large interval of order $\sqrt{U|\ln a|/\bar{U}\pi^2\rho_0^2}$. The FLEX solution differs only in that $\bar{U} = U$. The semi-elliptic form of the density of states in high frequencies is hence universal for one-particle self-consistent theories. The Hubbard satellite bands are completely smeared out. The reason for the nonexistence of the satellite peaks lies in the behavior of the real part of the self-energy in the low-frequency region. We compared the non-self-consistent and self-consistent solutions in Fig. 5. We can see that the sharp low-frequency structure of the real part of the self-energy is significantly smoothed and the peaks are broadened by the one-particle self-consistency. Most importantly, the height of the peaks near the Fermi energy is so much lowered that $|\omega| > |\Re\Sigma(\omega)|$. Only if this condition is broken, as is the case in the non-self-consistent solution, satellite peaks emerge.

V. CONCLUSIONS

We presented a construction of a universal analytic impurity solver reliably interpolating between the weak (Fermi liquid) and strong (Kondo) coupling metallic

regimes. The approximation is a simplification of two-channel parquet equations where the bounded irreducible vertex is replaced by a static effective interaction and only the low-frequency singular vertex is kept dynamical. Such a procedure is justified in the critical region of the metal-insulator transition where the low-frequency asymptotics of the singular two-particle vertex becomes dominant. We set with our construction the minimal necessary conditions that must be fulfilled to reproduce the Kondo exponential scale. The Kondo behavior is observed in an approximate solution of SIAM if the low-frequency singularity in the two-particle vertex dominates the dynamics and when electron-hole and electron-electron multiple scatterings are self-consistently mixed in a balanced way.

We analyzed two versions of the parquet approximation. In the first one, we used the Hartree one-electron propagators in the parquet equations for the two-particle irreducible vertices and the Schwinger-Dyson equation for the self-energy. In the second one we used the fully renormalized one-particle propagators. Although the latter construction contains more Feynman diagrams renormalizing the self-energy, its results are less reliable than the results of the former approach. This conclusion is not new and is also understandable.^{11,16} Renormalizations due to the one-particle self-consistency unrealistically smear and unfold the low-frequency structure of the self-energy. Consequently, the high-frequency features of the one-particle propagator are washed out and no Hubbard satellite bands can be observed.

One-particle self-consistency is standardly demanded in order to guarantee conservation laws and thermodynamic consistency. It is, however, not a necessary condition for approximations to be conserving. Conservation laws are guaranteed in any theory with an approximate self-energy functional containing physical external sources. These sources are then used to generate the desired physical quantities via linear response theory. On the other hand, theories aiming at a description of critical phenomena such as magnetic phase transitions or a metal-insulator transition must be self-consistent in some way. Self-consistency is necessary for any theory to

handle singularities. Since singularities in models with itinerant electrons emerge only at the two-particle level in Bethe-Salpeter equations, we must introduce a two-particle self-consistency. The parquet construction offers a very natural way to reach this goal and to treat singularities in the Bethe-Salpeter equations appropriately. One-particle self-consistency influences the critical behavior of the two-particle vertex, but it does not offer any direct control of singularities in the Bethe-Salpeter equations. It can neither guarantee integrability of singular vertices nor is capable to reproduce the correct critical behavior in the Kondo regime. When used in the parquet approach, the one-particle self-consistency interferes in the control of the two-particle singularities from the Bethe-Salpeter equations achieved by the two-particle self-consistency. The one-particle self-consistency can hence be used only when appropriately compensated so that it does not significantly affect the two-particle criticality. This is, however, not the case in the parquet approximation and the non-self-consistent one-particle propagators deliver better results than the self-consistent ones.

To conclude, we derived a global approximation that is analytically tractable, sufficiently simple, and universal. It can be used in a number of physically interesting situations, including realistic (multi orbital), material specific models as kind of a mean-field theory for models with strong local electron interaction. It may stand as an alternative to a recently proposed impurity solver for the strong-coupling regime.¹⁸ Unlike the solver from Ref. 18 our approximate scheme reproduces correctly the Kondo strong-coupling regime.

Acknowledgments

This research was carried out within a project AVOZ10100520 of the Academy of Sciences of the Czech Republic and supported in part by Grant No. 202/04/1055 of the Grant Agency of the Czech Republic.

-
- * Electronic address: janis@fzu.cz, august@fzu.cz
¹ A. M. Tsvelik and P. B. Wiegmann, *Adv. Phys.* **32**, 453 (1983).
² E. H. Lieb and F. Y. Wu, *Phys. Rev. Lett.* **20**, 1445 (1968).
³ A. Georges, G. Kotliar, W. Krauth, and M. Rozenberg, *Rev. Mod. Phys.* **68**, 13 (1996).
⁴ T. Pruschke and N. Grewe, *Z. Physik B* **74**, 439 (1989).
⁵ M. Jarrell, *Phys. Rev. Lett.* **69**, 168 (1992).
⁶ A. C. Hewson, *The Kondo Problem to Heavy Fermions* (Cambridge University Press, Cambridge 1993).
⁷ R. Bulla, *Phys. Rev. Lett.* **83**, 136 (1999).
⁸ N. E. Bickers and D. J. Scalapino, *Ann. Phys. (N. Y.)* **193**, 206 (1998).
⁹ R. A. Weiner, *Phys. Rev. B* **4**, 3165 (1971).

- ¹⁰ N. E. Bickers and S. R. White, *Phys. Rev. B* **43**, 8044 (1991).
¹¹ V. Zlatić and B. Horvatić, *Phys. Rev. B* **28**, 6904 (1983).
¹² V. Janiš, *Phys. Rev. B* **60**, 11345 (1999).
¹³ C. X. Chen and N. E. Bickers, *Solid. State Commun.* **82**, 311 (1992).
¹⁴ D. R. Hammann, *Phys. Rev.* **186**, 549 (1969).
¹⁵ G. Baym, *Phys. Rev.* **127**, 1391 (1962).
¹⁶ Y. M. Vilk and A. M. S. Tremblay, *J. Phys. (Paris)* **7**, 11309 (1997).
¹⁷ H. Suhl, *Phys. Rev.* **171**, 561 (1967).
¹⁸ X. Dai, K. Haule, and G. Kotliar, *Phys. Rev. B* **72**, 045111 (2005).